

Prediction and Measurement of Fatigue Lifetime Distributions for Elastomeric Biomaterials

K. P. GADKAREE* and J. L. KARDOS, *Materials Research Laboratory and Department of Chemical Engineering, Washington University, St. Louis, Missouri 63130*

Synopsis

Synthetic polymer biomaterials being considered for cardiovascular applications must perform under conditions of large cyclic deformations for long lifetimes. In designing with these materials and eventually qualifying them clinically, it would be extremely helpful to be able to predict the fatigue lifetimes accurately and reliably. In this article a calculational format is presented which predicts the lifetime distribution function for elastomeric sheets undergoing tension-tension fatigue. From a knowledge of the intrinsic tensile strength distribution and the effect of an "equivalent" edge flaw size on the tensile strength, the inherent flaw size distribution is determined. A tearing energy concept is utilized to determine the flaw growth law constants. Each of these three short-term tests provides a pair of constants which, taken together, permit calculation of the fatigue lifetime distribution. When compared using Kolmogoroff statistics, experimental tensile-tensile fatigue results at 0.01 cps agreed well with the theoretically predicted lifetime distribution function.

INTRODUCTION

Synthetic polymer biomaterials are often asked to perform under conditions of large cyclic deformations for long lifetimes. Typical of such applications are left ventricular assist (LVA) pump bladders, heart valve components, and vascular grafts. Two important clinical problems that could arise in the application of these materials are excessive creep and fatigue failure. Creep has been reported in Teflon vascular grafts,¹ and fatigue cracking and failure is certainly an important design consideration in LVA pump bladders. In designing with these materials and eventually qualifying them for clinical usage, it is necessary to be able to predict the fatigue lifetimes accurately and reliably. To be sure, these materials must be biologically compatible; but even the most perfectly biocompatible material will not be qualified for structural use in humans unless its mechanical longevity can be proven from an accurate data base.

The nature of the fatigue problem is complicated by the statistical spread of cycles-to-failure data at any one stress level. If fatigue life is to be reliably predicted, the statistical nature of the failure must be examined. Curiously, there has not been much effort to do this for polymers,^{2,3} although fatigue laws involving two-parameter Weibull distributions have often been employed in describing fatigue of metals and reinforced plastics.⁴

Usually, the problem of life prediction is treated in a deterministic way.

* Present address: Corning Glass Works, Corning, NY 14830.

A crack growth law of the form

$$\frac{dc}{dn} = A(\Delta K)^b \quad (1)$$

or

$$\frac{dc}{dn} = AT^m \quad (2)$$

is determined experimentally, and, since the parameters K and T are known in terms of c , the crack length, the above equations are integrated between limits of c_0 to c_c , where c_c gives the critical crack size at which catastrophic failure occurs, and 0 to n , where n is lifetime in cycles. This has been the approach adopted in the studies on elastomers⁵⁻⁸ and most investigations of plastics³ and reinforced plastics.⁹ This does not help in explaining the scatter observed in the lifetime of specimens which look exactly the same and are subjected to the same conditions.

It is now an accepted fact that fatigue failure initiates at preexisting flaws. These flaws grow due to fatigue loading, and catastrophic failure takes place as the critical size is reached. Thus, knowing the distribution of initial flaw sizes and the fatigue law for flaw propagation, the distribution of flaw sizes after n cycles can be determined, and the probability of failure calculated.

Experimentally, both the distribution of breaking strengths and the relationship between breaking strength and size of a critical flaw must first be found. Using this information, the distribution of initial flaw sizes can be determined. The flaw growth law is then characterized experimentally. Information from these three types of experiments is then used to obtain the fatigue lifetime distribution function.

In the following the details of the theoretical approach are described and the predicted fatigue lifetime distributions compared with experimental data for a segmented polyetherurethane material.

THEORETICAL DEVELOPMENT

Initial Flaw Size

Every solid body contains flaws as points of weakness due to heterogeneities of composition or structure. In addition, because of the presence of sharp corners, nicks, cuts, scratches, and embedded dirt particles or other sharp inclusions, applied stresses are magnified in certain regions of the body so that they greatly exceed the mean applied stress. The failure process will begin at such a site where the local stress exceeds a critical level and the small flaw starts to grow as a microcrack. These initial flaw sizes will be different in different specimens in a given population, so different lifetimes will result for different specimens under fatigue conditions. It is necessary, then, to determine this flaw size distribution. For a semitransparent biomaterial, there are two possible approaches to do this. The first

and most obvious is to examine the specimen under an optical microscope and measure the size and shape of different flaws. The failure process should start at the largest and sharpest flaw but this may not always be true. There may be several different flaws present around a given flaw, and their stress fields will interact. Thus, the failure process may start from a small flaw around which there are several stress concentrators rather than from a larger flaw around which there are few other stress concentrators.

Another way to measure flaws is to use a "hypothetical flaw concept." For brittle materials, the well-known Griffith relationship between breaking strength and the size of an artificially introduced sharp flaw or crack is

$$\sigma_b = (2Es/\pi c)^{1/2} \quad (3)$$

where c is the crack size and s is the surface energy. This relationship has been verified for metals, and for brittle polymers by Berry,⁷ although, in the case of polymers, s , the surface energy, has to be replaced by γ , a characteristic energy. This equation has been assumed to be valid for elastomers also.¹⁰

It is, however, not necessary to use the above equation. As is shown below, a relationship can be derived between breaking stress and flaw size for elastomers by utilizing the tearing energy theory,¹¹ which has been verified for several different elastomers.^{5,6,8,12} Consider a specimen with an edge flaw of length c . The specimen when loaded will break at a critical value of tearing energy (T_c), which is characteristic of the material, rate of tearing, and temperature. This T_c is defined by

$$T_c = 2KUc \quad (4)$$

where K is a constant, which varies weakly with strain, U is the strain energy density defined by $U = \int_0^\epsilon \sigma d\epsilon$, and c is the flaw length; hence,

$$T_c = 2K \cdot \int_0^\epsilon \sigma d\epsilon \cdot c \quad (5)$$

Now, if $\sigma = A\epsilon^n$ (a nonlinear stress strain relationship), it can easily be shown¹³ that

$$\sigma_b = \beta/c^{n/1+n} = M/c^N \quad (6)$$

where

$$M = \alpha^N \quad \text{and} \quad \alpha = \frac{T_c}{(1/A)^{1/n} \cdot [1/(n+1)] \cdot 2K}$$

For linear elastic material when $n = 1$,

$$\sigma_b \propto \frac{1}{c^{1/2}}$$

which is the Griffith criteria. Since most elastomers have a nonlinear stress strain curve, eq. (6) should be used rather than the Griffith criteria.

Equation (6) thus supplies a very simple means of determining the needed flaw size distribution. Various small sharp flaws can be introduced in specimens and the specimens then broken at a specified strain rate. Equation (6) will be satisfied if a straight line results upon plotting σ_b vs. c on a log-log scale, and values of M and the exponent N may then be obtained.

Subsequently, several more specimens can be broken at the same strain rate as before. Using eq. (6), the equivalent hypothetical flaw size does not necessarily correspond to any actual flaw size in the specimen, but may be thought of as that single flaw size which would have the same effect as multiple smaller interacting flaws. Thus, if the breaking strength distribution is known, the equivalent flaw size distribution in a given specimen's population can be found using probability theory methods.

Initial Flaw Size Distribution

Let us assume that the probability distribution of breaking strengths is given by a normal distribution function

$$f(\sigma_b) = \frac{1}{\sigma\sqrt{2\pi}} \exp\left[-\frac{1}{2}\left(\frac{\sigma_b - \mu}{\sigma}\right)^2\right] \quad (7)$$

where μ and σ^2 are the mean and variance of the distribution and σ_b is the breaking strength. To determine the probability distribution of flaw sizes in this population, eq. (6) and transformation of variables is used (see the Appendix) to obtain

$$f(c) = \frac{MN}{\sigma\sqrt{2\pi} c^{1+N}} \exp\left\{-\frac{1}{2}\left[\frac{M}{c^N} - \mu\right]^2 / \sigma^2\right\} \quad (8)$$

Thus, the distribution of hypothetical flaw sizes in a given specimen population is obtained. A similar procedure can be used for any other distribution function.

Flaw Growth

Fatigue flaw growth in elastomers above a characteristic tearing energy T_0 is correlated by an equation of the type

$$\frac{dc}{dn} = AT^b \quad (9)$$

where A and b are constants depending on experimental conditions and the material. T , the tearing energy, is given for an edge crack by $T = 2KUc$ where K is a numerical constant and U is the area under the stress-strain curve. Hence eq. (9) becomes

$$\frac{dc}{dn} = A(2KUc)^b \tag{10}$$

$$\frac{dc}{c^b} = A(2KU)^b dn$$

Integrating this equation between the limits c_0 to c (initial flaw size and flaw size after n cycles, respectively) and 0 to n , where n is the number of cycles and $z = A(2KU)^b(b - 1)n$ yields

$$c_0 = [z + c^{-(b-1)}]^{-1/(b-1)} \tag{11}$$

Now eq. (8) gives the probability distribution of the initial crack sizes, c_0 's. So, the probability distribution of crack sizes after n cycles will be

$$f(c_n) = \frac{MN}{2} \frac{(z + c^{-(b-1)})^{-b/(b-1)} c^{-b}}{(z + c^{-(b-1)})^{-(1+N)/(b-1)}} \tag{12}$$

$$\times \exp \left\{ -\frac{1}{2} \left[\left(\frac{M}{(z + c^{-(b-1)})^{-N/(b-1)}} - \mu \right) / \sigma \right]^2 \right\}$$

Lifetime Distribution

The distribution function $f(c_n)$ gives the probability distribution of flaws in specimens after n fatigue cycles under a given set of experimental conditions. The probability that a specimen will contain a flaw greater than the critical size, at which catastrophic failure takes place is given by

$$P_r(f) = 1 - P_r(s) \tag{13}$$

where

$$P_r(s) = \int_0^{a_c} f(c_n) dc_n \tag{14}$$

where a_c is the critical flaw size. Thus, by calculating $P_r(f)$ at various values of n and plotting $P_r(f)$ vs. n , one can determine what the probability of failure is for a given specimen under given experimental conditions.

A simplification can be introduced based on the assumption that the final length of the crack (i.e., the length when the specimen fails) is very much larger than the initial crack length, $c_0 \ll c_c$. In this case eq. (11) can be rewritten as

$$\frac{1}{c_0^{b-1}} = A(2KU)^b(b-1)n \tag{15}$$

From this equation, the probability distribution of fatigue lives can be derived directly. Equations (15) and (8) give the fatigue life distribution as

$$f(n) = \frac{MN}{\sigma\sqrt{2\pi}} \left(\frac{1}{b-1} \right) \frac{n^{(N+1-b)/(b-1)}}{[1/A(b-1)(2KU)^b]^{N/(b-1)}} \quad (16)$$

$$\times \exp \left\{ -\frac{1}{2} \left[\left(\frac{Mn^{N/(b-1)}}{[1/A(b-1)(2KU)^b]^{N/(b-1)}} - \mu \right) \sigma \right]^2 \right\}$$

Thus, eq. (16) can provide the fatigue lifetime distribution functions under given experimental conditions without carrying out any fatigue tests at all, if the six constants (M , N , μ , σ , A , b) are known.

EXPERIMENTAL

Materials

Experiments were carried out to verify the above procedure for elastomeric biomaterials. The material used was Biomer, a segmented polyetherurethane polymerized by Ethicon, Inc. and centrifugally cast into 30-mil-thick sheets by Thoratec, Inc.

The casting was accomplished by applying a 20 wt % solution of Biomer in N,N -dimethylacetamide (DMAC) to the inside of a rotating (544 rpm) aluminum cylinder closed at one end and lined with a 5-mil Mylar film. Filtered warm air was blown over the film to remove most of the DMAC, and the sheet then removed and the Mylar stripped off. The sheets were then dried for 2 h at 70°C, extracted in distilled water at 80°C for 4 h, and then vacuum-dried. Dog-bone specimens were punch-cut from these sheets with a hand mallet and die. The central narrow portion of the specimens was 1 in. long and 0.26 in. wide. The thickness of every specimen was measured at four places on the narrow portion. Only specimens with uniform thickness (± 0.25 mils) were used for the experiments. Two types of experiments were carried out at room temperature. First, determination of the tensile strength with and without a cut flaw in the specimens was carried out in an Instron testing machine. Second, fatigue and crack propagation experiments were carried out on an MTS electrohydraulic testing machine. Experimental procedures are described below in detail.

Strength Determination without a Cut Flaw

In an effort to determine the relationship between breaking strength and flaw size, several specimens were examined at about $1000\times$ magnification under an optical microscope. Flaws in the specimens were clearly visible and were mapped, including their shapes and sizes, for each specimen. These specimens were then broken in uniaxial tension in an Instron testing machine at a crosshead speed of 5 in./min, using air-pressure grips with sandpaper faces. The place at which the specimen broke was marked on the map. The largest and sharpest flaw was then located in that region, and it was assumed that failure initiated at this flaw. A log-log plot of breaking strength vs. flaw size determined thus did not yield any correlation. It was then postulated that the actual flaw size cannot be used because of interacting stress fields from several nearby flaws, which apparently change the

effective flaw size. Nonetheless, these experiments, along with the controlled cut flaw tests, can yield sufficient information to obtain the effective flaw size distribution.

Strength Determination with a Cut Flaw

In these experiments, a small sharp edge cut was introduced halfway up the gage length of the specimen with the aid of an optical microscope. Care was taken to make sure that the cut was perpendicular to the side of the specimen and therefore had the same depth when measured from front or back. Cuts were introduced in several specimens, and the cut length was measured under an optical microscope with an accuracy of $\pm 12.2 \mu\text{m}$, i.e., 0.00048 in. These specimens were then broken in tension in an Instron testing machine at 5 in./min crosshead speed (5 in./in. \cdot min⁻¹). The breaking strength was then plotted against cut length on log-log paper.

Dynamic Tests

The crack propagation and fatigue experiments were carried out on an MTS closed-loop electrohydraulic testing machine. The load range required in these experiments was from 5 to 15 lb. Since the machine was designed for use in much higher load ranges, and since the load cell used here was in the 0–50 lb range, it was extremely sensitive and picked up the machine frame vibrations which were transmitted to the controller affecting the actuator movement as unwanted feedback. To dampen these vibrations, a 4-in. cubic block of wood was attached to the load frame, and the load cell was attached to this block through a foam packing spacer between the block and the frame. This arrangement made it possible to use the machine in load control without feedback noise.

Flaw Propagation and the Tearing Energy Relation

In order to examine the flaw growth law, a small, sharp edge cut was introduced in the specimen with a razor blade. The specimen was then mounted in sandpaper-lined grips of an MTS testing machine and stressed sinusoidally in tension. A traveling microscope was used to measure the length of the crack at various low numbers of cycles. For each particular frequency, experiments were done for at least four to five different maximum stress levels. Frequencies of 1 cps, 0.1 cps, and 0.01 cps were used. Only the results of 0.01 cps are reported here because fatigue experiments were carried out at that frequency.

The crack growth experiments provide part of the data needed for the plot of dc/dn vs. T . Another problem encountered at this point involved calculation of U , the strain energy density which is needed to calculate the tearing energy T . The value of U is equal to the area under the true stress–true strain curve. Now, for a given stress level (i.e., given extension) the flaw propagation or fatigue specimens clearly stretch at different rates when cycling at different frequencies. If the true stress–true strain curves change appreciably with extension rate, different stress–strain curves must be used for calculating U at different frequencies.

To study these rate effects, engineering stress–engineering strain curves were obtained on an Instron testing machine at 2, 12, and 20 in./in. · min⁻¹. It was found that there was negligible difference between them, and so a single value of U was used for experiments done at different frequencies in this extension rate range.

Fatigue Lifetimes

Fatigue experiments were carried out at a frequency of 0.01 cps at 1556 psi, 900 psi, and 750 psi maximum engineering stress and 0 psi minimum stress under cyclic sinusoidal conditions. Each stress level results in a different value of U , and so a different distribution function of fatigue lifetimes will result at different stress levels. The predicted lifetime distribution function was compared with the experimental results for goodness of fit.

RESULTS AND ANALYSIS

The results are analyzed sequentially according to the development and utilization of the theory. Chronologically, one must first measure the intrinsic breaking strength without an induced flaw and then the breaking strength with an induced flaw or cut. Next, the crack propagation law must be characterized, and finally, the fatigue lifetime predictions must be checked against the experimental fatigue results.

Breaking Strength Distribution

Table I shows the values of pristine breaking strengths obtained, arranged in increasing order for a particular lot of samples. First, the sample lot was tested using the χ^2 goodness of fit test to see if it was from a normal population. Maximum likelihood estimates were made for the sample mean μ and standard deviation σ and are shown in Table I.

The data were then grouped into five different classes, the frequency of appearance of the data in each class was counted, and the theoretical probabilities were generated from standard normal distribution tables. The critical X^2 parameters were then calculated at $\alpha = 0.05$ (95% confidence level). The calculations showed that there was no reason to reject the hypothesis that the breaking strength data follow a normal distribution with a mean $\mu = 5874.58$ and a standard deviation $\sigma = 199$ psi.

TABLE I
Breaking Strengths without Cut (psi) for a Sample Set of 31 Specimens^a

$n = 31$									
5468,	5528,	5528,	5616,	5631,	5649,	5649,	5649,	5738,	5793,
5835,	5835,	5889,	5906,	5906,	5921,	5937,	5937,	5937,	5937,
5975,	5978,	5997,	6025,	6072,	6089,	6100,	6100,	6140,	6140,
6207									

^a $\mu = \text{mean} = 587$; $\sigma = \text{standard deviation} = 199$.

Thus, the distribution of breaking strengths for this particular lot of uncut specimens may be written as

$$f(\sigma_b) = \frac{1}{\sqrt{2\pi} (199)} e^{-\frac{1}{2}[(\sigma - 5875)/199]^2} \tag{17}$$

where σ_b is the breaking strength.

Dependence of Breaking Strength on Flaw Size

The next step in developing the fatigue life prediction involves determining what the breaking strength dependency is on the effective flaw size. Precision cuts were introduced, and specimens broken in tension. The results of plotting these data on a log-log plot are shown in Figure 1 along with a least-squares-fit straight line. The values of constants M and N in the relationship

$$\sigma_b = M/c^N$$

were determined to be

$$M = 608, \quad n = 0.39$$

Hence, the relation

$$\sigma_b = 608/c^{0.39}$$

yields the particular flaw size effect on strength for this population of Biomer samples. Following the theoretical development explained earlier, the distribution of flaw sizes becomes

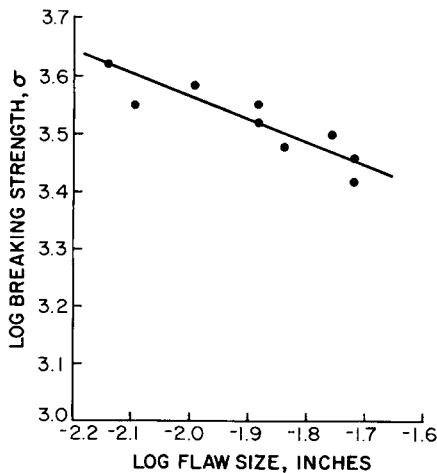


Fig. 1. Correlation between breaking strength and flaw size utilizing eq. (6); $M = 608$, $N = 0.39$.

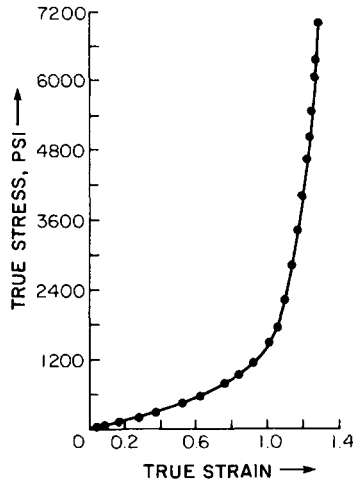


Fig. 2. True stress vs. true strain curve. This curve is independent of the strain rate between 2 and 20 min^{-1} .

$$f(c) = \frac{608(0.39)}{199\sqrt{2\pi c^{1.89}}} e^{-\frac{1}{2}[(608/c^{0.39} - \mu)/199]^2} \quad (18)$$

Cut Growth Experiments—The Flaw Propagation Law

The next step in generation of a fatigue lifetime distribution function involves determining how the flaws will grow to produce a critical size flaw which, in turn, produces failure. Flaw (cut) growth experiments were carried out as described before. It was found that a relationship of the type

$$\frac{dc}{dn} = AT^b$$

where $T = 2KUc$, correlates the results extremely well.

The stress-strain curve shown in Figure 2 was used for calculation of the

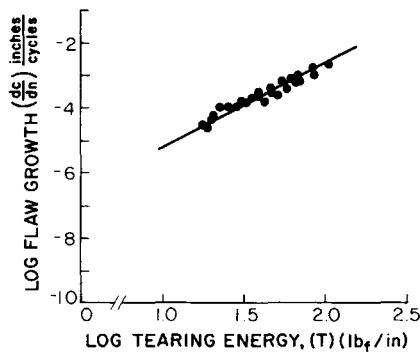


Fig. 3. Least squares fit of tearing energy-crack growth law correlation at a frequency of 0.01 cps.

energy U . The relationship between cut growth rate and the tearing energy at 0.01 cps is shown in Figure 3.

For 0.01 cps, the values of the crack growth law constants are

$$A = 1.778 \times 10^{-8}, \quad b = 2.5$$

Fatigue experiments were carried out at maximum stresses of 1556, 900, and 750 psi. Calculations of the predicted lifetime distribution function for each stress level are shown below.

Lifetime Distribution Function

The last step in the predictive format involves utilizing the information from the strength, the strength-with-a-flaw, and the crack propagation experiments to predict the fatigue lifetime distribution. These predictions for each of three maximum stress levels are summarized below for a frequency of 0.01 cps.

1556 psi. From the crack-growth experiments, it is known that at this stress level

$$K = 1.6, \quad b = 2.5$$

$$A = 1.778 \times 10^{-8}, \quad U = 1208.3 \text{ lb}_f/\text{in.}^2$$

Substituting these values into eq. (16) along with the values for σ and μ as well as M and N , we obtain,

$$f(n) = \frac{0.7298}{n^{0.74}} e^{-\frac{1}{2}(7.036n^{0.2599} - 29.50)^2} \tag{19}$$

which is the lifetime distribution function at 1556 psi.

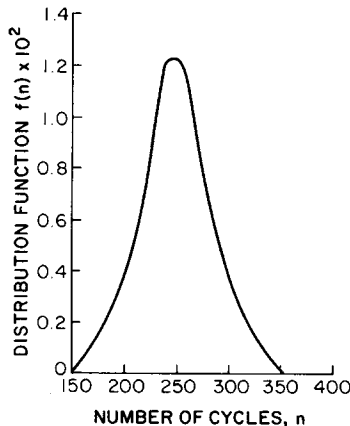


Fig. 4. Distribution function for uniaxial tensile fatigue lifetimes of Biomer sheet at a maximum sinusoidal stress of 1556 psi.

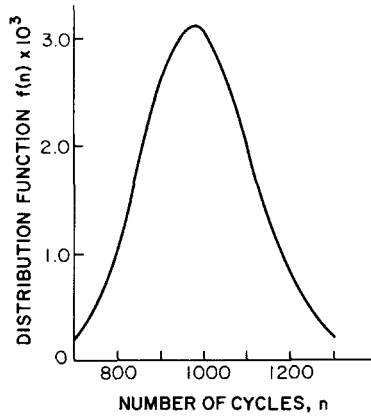


Fig. 5. Distribution function for uniaxial tensile fatigue lifetimes of Biomer sheet at a maximum sinusoidal stress of 750 psi.

900 psi. The values of A , b , σ , μ , M , and N are the same as before, $K = 1.65$ and $U = 790.8 \text{ lb}_f/\text{in.}^2$; hence

$$f(n) = \frac{0.5653}{n^{0.74}} e^{-\frac{1}{2}(5.450n^{0.260} - 29.50)^2} \quad (20)$$

750 psi. A , b , σ , μ , M , and N are the same as before: $K = 1.68$ and $U = 663.3 \text{ lb}_f/\text{in.}^2$. Thus,

$$f(n) = \frac{0.5101}{n^{0.74}} e^{-\frac{1}{2}(4.918n^{0.260} - 29.50)^2} \quad (21)$$

Equations (19)–(21) thus give the predicted lifetime distributions for 1556, 900, and 750 psi maximum stress levels, respectively. These distributions are plotted in Figures 4–6.

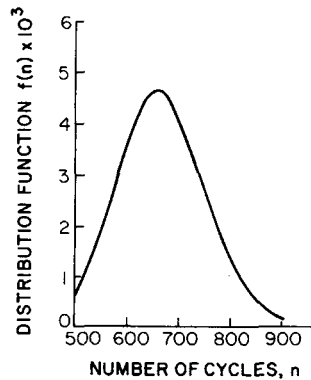


Fig. 6. Distribution function for uniaxial tensile fatigue lifetimes of Biomer sheet at a maximum sinusoidal stress of 900 psi.

Fatigue Experiments

Fatigue experiments were carried out to see whether the experimentally obtained values of fatigue lives fit the predicted distributions. Since completely specified distribution functions are given by eqs. (19)–(21), a Kolmogoroff test of goodness-of-fit was used.¹⁴ This test is particularly applicable to a small number of samples. To apply the Kolmogoroff test, the sample cumulative distribution function (cdf), as well as the postulated distribution value, must be evaluated for each distinct observation. In comparing the χ^2 test with the Kolmogoroff test, it is noteworthy that the latter is computationally simpler, does not lose information by grouping of data, and applies directly to small samples. On the other hand, the χ^2 test is applicable to a composite hypothesis (i.e., when parameters need to be estimated from the data).

The Kolmogoroff statistics test measures the maximum absolute deviation of the sample cdf from the corresponding value obtained from the postulated distribution function. Ten fatigue experiments were completed at 1556 psi maximum sinusoidal stress. Table II summarizes the Kolmogoroff statistical calculations.

As can be seen from the results of Table II, the maximum deviation is 0.364. From the tables at $\alpha = 0.1$ and $N = 10$ the critical value is 0.368. Since the highest value is less than the critical value, there is no reason to reject the hypothesis that eq. (19) does describe the lifetime distribution at 1556 psi at $\alpha = 0.1$ (90% confidence limit). The value of $F(n)$ in the table is obtained by integrating eq. (19) within the limits 0 to x , where x is the value of the lifetime. The integration was done using a 16-point Gauss–Legendre quadrature format on a programmable H-P calculator.

A similar analysis was done at 900 psi and 750 psi and the results showed that eqs. (20) and (21) do indeed describe the fatigue lifetime distribution functions at $\alpha = 0.1$.

TABLE II
Summary of Kolmogoroff Statistical Test Calculations

Class	Observed value	Frequency n_i	Cumulative frequency n_i	Sample cdf $\Sigma n_i/n$	$F(n)$	Absolute deviation $F(n) - \text{sample cdf}$
1	114	1	1	0.1	3.183×10^{-8}	0.1
2	146	1	2	0.2	0.00007	0.19993
3	168	1	3	0.3	0.00216	0.29784
4	195	1	4	0.4	0.03588	0.36412
5	221	1	5	0.5	0.18822	0.31178
6	279	1	6	0.6	0.81718	0.21718
7	287	1	7	0.7	0.87073	0.17073
8	331	1	8	0.8	0.98969	0.18969
9	377	1	9	0.9	1.00055	0.10055
10	478	1	10	1.0	1.00085	0.00085

CONCLUSIONS

1. A format has been developed to predict the fatigue lifetime distribution function of an elastomeric biomaterial from short-term experimental data. At a confidence level of 90%, the predicted lifetime distributions adequately describe the limited experimental data as measured by the Kolmogoroff statistical test.

2. Three types of experiments have to be done before the distribution function can be estimated; these are (1) breaking strength experiments with a cut in the specimen, (2) breaking strength experiments without a cut in the specimen, and (3) flaw growth experiments. Each type of experiment gives a pair of constants; thus six experimentally determined constants are required for obtaining the distribution function.

We are grateful for the support of this work by the National Heart, Lung, and Blood Institute, Division of Heart and Vascular Diseases, Devices and Technology Branch Under Contract No. NO1-HV-02910.

APPENDIX: INITIAL FLAW SIZE DISTRIBUTION

Let us assume that the probability distribution of breaking strengths is given by a normal distribution function

$$f(\sigma_b) = \frac{1}{\sigma\sqrt{2\pi}} \exp\left[-\frac{1}{2}\left(\frac{\sigma_b - \mu}{\sigma}\right)^2\right] \quad (22)$$

where μ and σ^2 are the mean and variance of the distribution and σ_b is the breaking strength. To determine the probability distribution of flaw sizes in this population using eq. (6), the following theorem in probability theory is used.

Theorem: If X is a continuous random variable with a probability distribution function $f(x)$ and $Y = u(X)$ defines a one-to-one correspondence between the values of X and Y , so that equation $y = u(x)$ can be uniquely solved for x in terms of y , say, $x = w(y)$, then the probability distribution of Y is

$$g(y) = f[w(y)]|J| \quad (23)$$

where $|J| = w'(y)$ and is called the Jacobian of the transformation.

Let us write eq. (6) as $\sigma_b = M/c^N$. Then, using the above theorem, the probability distribution of flaw sizes becomes

$$f(c) = \frac{1}{\sigma\sqrt{2\pi}} \exp\left[-\frac{1}{2}\left(\frac{M/c^N - \mu}{\sigma}\right)^2\right] |J| \quad (24)$$

where

$$|J| = \frac{d}{dc} \left(\frac{M}{c^N}\right) = |M[-Nc^{-N-1}]| = \left|-\frac{MN}{c^{1+N}}\right| = \frac{MN}{c^{1+N}}$$

so that

$$f(c) = \frac{1}{\sigma\sqrt{2\pi}} \exp\left[-\frac{1}{2}\left(\frac{M/c^N - \mu}{\sigma}\right)^2\right] \frac{MN}{c^{HN}} \quad (25)$$

$$f(c) = \frac{MN}{\sigma\sqrt{2\pi}c^{1+N}} \exp\left\{-\frac{1}{2}\left[\left(\frac{M}{c^N} - \mu\right) / \sigma\right]^2\right\}$$

Thus, the distribution of hypothetical flaw sizes in a given specimen population is obtained.

References

1. C. D. Campbell, D. H. Brooks, M. W. Webster, R. P. Bondi, J. C. Lloyd, M. F. Hynes, and H. T. Bahnson, *Surgery*, **79**, 491 (1976).
2. J. A. Manson and R. W. Hertzberg, *Crit. Rev. Macromol. Sci.*, **1**, 433 (1973).
3. R. W. Hertzberg and J. A. Manson, *Fatigue of Engineering Plastics*, Academic, New York, 1980.
4. J. M. Whitney, *Fatigue of Fibrous Composite Materials, ASTM STP 723*, American Society for Testing and Materials, Philadelphia, 1981, p. 133.
5. A. N. Gent, P. B. Lindley, and A. G. Thomas, *J. Appl. Polym. Sci.*, **8**, 453 (1974).
6. G. J. Lake and P. B. Lindley, *J. Appl. Polym. Sci.*, **8**, 107 (1974).
7. J. P. Berry, *J. Polym. Sci.*, **50**, 107 (1961).
8. R. E. Whittaker, *J. Appl. Polym. Sci.*, **18**, 2339 (1974).
9. A. T. DiBenedetto and G. Salee, *Proceedings of the 34th Antec, Society of Plastics Engineers*, Atlantic City, 1976, p. 103.
10. A. N. Gent, *Science and Technology of Rubber*, F. R. Eirich, Ed., Academic, New York, 1978.
11. R. S. Rivlin and A. G. Thomas, *J. Polym. Sci.*, **10**, 291 (1953).
12. H. W. Greensmith, *J. Appl. Polym. Sci.*, **8**, 113 (1964).
13. K. P. Gadkaree, "Prediction and Measurement of the Durability and Reliability of Elastomeric Biomaterials," D.Sc. thesis, Washington University, May 1980.
14. K. V. Bury, *Statistical Models in Applied Science*, Wiley, New York, 1975.

Received October 25, 1983

Accepted March 26, 1984